Ion oxide conductor as a catalytic membrane for selective oxidation of hydrocarbons

C. Courson, B. Taouk * and E. Bordes **

Département de Génie Chimique, Université de Technologie de Compiègne, BP 20529, 60205 Compiègne Cedex, France

Received 9 August 1999; accepted 28 March 2000

A catalytic membrane reactor using ion-oxide conductors as catalysts is experienced in selective oxidative dimerization of propene to C_6-dimers. Structural and textural properties, catalytic and non-catalytic reactivities of M-doped Bi_2O_3 (M = La, Ce, Eu, Er, V, Nb) are studied. TGA experiments show that dopants increase the rates of reduction and reoxidation of Bi_2O_3, but that the reoxidation of the catalysts is rate limiting. During catalysis, the best yields in 1,5-hexadiene and benzene are obtained with cerium-doped Bi_2O_3.

Keywords: doped bismuth oxide catalyst, membrane reactor, catalytic membrane, ion-oxide conductor, redox behavior, oxidative coupling of propene

1. Introduction

Applications of membrane reactors are found in several fields, mainly in biotechnology and chemical processes [1]. Their interest lies in the possibility of coupling the reaction to the separation of products (or reactants). Catalytic membrane reactors (CMR) are more and more investigated. In the field of petrochemistry, studies on dehydrogenation and on oxidation reactions are flourishing, as shown by symposia dedicated to this subject. The membrane can be passive, permeaselective or not, and the catalyst is generally supported on it. Cases where the membrane is active by itself are less numerous. Recently, dense oxide membrane reactors have drawn attention for oxidation reactions. Oxygen-ion conducting membranes can be operated with air as an economical source of oxygen, without the drawback of nitrogen ballast. Perovskite-type materials are now proposed for conversion of natural gas to syngas or to C_{2+} hydrocarbons [2–4].

The role of ionic conductivity in catalysis has been already our concern. About ten years ago, copper and silver cationic conductors of the NASICON family were examined in the selective oxidation of propene to acrolein [5–7]. Recently we have studied lanthanum-doped bismuth oxide catalysts in a CMR configuration to perform the oxidative dehydrodimerization of propene to benzene [8]. At that time, the aim was to confirm the feasibility demonstrated by Di Cosimo et al. [9], and to examine the role of ion-oxide mobility in selective oxidation. Indeed, the oxygens of the selective oxidation catalysts are known to participate in the reaction according to the two-stepped kinetic mechanism proposed by Mars and van Krevelen [10]. The first step is the oxidation of the reactant molecule by surface lattice oxygen (i.e., O^{2-} oxygen ion in normal crystallographic position) of the oxidized form of the catalyst, and the second step is the reoxidation of the reduced catalyst by the cofed gaseous dioxygen (pure or in air). Depending on whether the rate-limiting step is the reduction or the reoxidation of the catalyst, and depending on the structure of the catalyst, the surface vacancies created during the first step can be replaced by oxide ions coming from the bulk by ionic diffusion. This is particularly the case of bismuth molybdates in the oxidation of propene to acrolein or acrylonitrile [11] and of vanadium pentoxide in oxidation of, e.g., *o*-xylene to phthalic anhydride [12]. A certain degree of ionic conductivity is therefore required in many cases [13,14].

The oxidative coupling of propene to 1,5-hexadiene and benzene has been already studied using bismuth-based mixed oxide catalysts in several types of reactor: fixed-bed reactor [9,15], pulse reactor [16–18] or sequential reactor [19,20]. As in the case of bismuth molybdate for mild oxidation of propene to acrolein [11], the first step of the reaction is the abstraction of a hydrogen atom from propene by an oxygen linked to bismuth [21,22]. Bismuth vanadate and some BIMEVOX (ME = Sr, Cu, Fe) which are solid solutions of metal in $Bi_4V_2O_{11}$ [23] have also been studied in the oxidative coupling of methane and oxidative dehydrogenation of propane [24]. The main drawback of Bi oxides is their poor stability on-stream because they are easily reduced, as shown by metallic bismuth occurring during the reaction. The principle of the catalytic membrane reactor (figure 1) using bismuth oxide as a dense membrane is an illustration of the Mars and van Krevelen mechanism: (i) on the reaction side, propene is oxidized by surface O^{2-} so that the surface is depleted and bulk O^{2-} diffuse to refill vacancies; and (ii) on the oxidation side, gaseous O_2 is first reduced and then the

* To whom correspondence should be addressed.
** Present address: Laboratoire de Catalyse, Université des Sciences et Technologies de Lille, Bât. C3, 59655 Villeneuve d'Ascq Cedex, France.

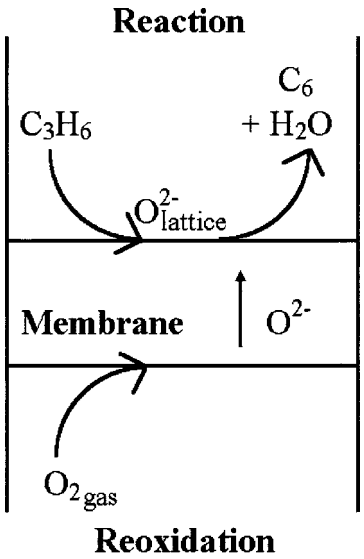

Figure 1. Schematic of the catalytic membrane reactor using ion-oxide conductor.

O^{2-} oxide ion diffuses towards the other side. The driving force is the oxidation of the hydrocarbon, and the mobility of O^{2-} depends on the ionic conductivity of the catalyst. Like in the case of the recirculating fluid solid reactor [25], the advantage of CMR is that oxygen (air) is not cofed with propene, which avoids the formation of by-products due to direct reactions between propene and oxygen.

Among the various allotropic forms of Bi_2O_3, γ and δ are the best ionic conductors, but they are stable at high temperature only (640 and 729 °C, respectively) [26]. These forms can be stabilized at room temperature by promoters modifying their reactivity, such as alkaline earths, lanthanides or transition metals. In the case of La-doped Bi_2O_3 used in a CMR configuration [8], a small amount of metallic bismuth was found after reaction. In order to improve the stability and to examine the influence of ionic conductivity on the reaction, other dopants (Ce, Eu, Er, V and Nb) have been used. The preparation of the catalysts, their structural characterization, reactivity in redox conditions and catalytic properties in CMR configuration are presented in this paper.

2. Experimental

2.1. Preparation of catalysts and of catalytic membranes

The solids were prepared by synthesis methods from literature [27–29]. The conditions and compositions are reported in table 1. Depending on the promoters, two methods were used. In the case of La and Ce, precursors were co-precipitated from aqueous nitrate solutions, the precipitate being then dried overnight at 110 °C [9]. The oxides Eu_2O_3, Er_2O_3, V_2O_5 and Nb_2O_5 were mechanically mixed in stoichiometric amount with Bi_2O_3. In all cases, the obtained solids were calcined in air at 3 °C min^{-1} heating rate for various periods and temperatures (table 1), and then cooled slowly to room temperature.

The catalytic membrane disks were obtained by pressing and sintering catalyst powders. 2 g of solid were used to make a 2 mm thickness and 13 mm diameter disk by compression (8 tons cm^{-2}). The disk was sintered in air at 800 °C during 16 h, and then sealed on the disk carrier to be inserted in the catalytic reactor with an adhesive ceramic paste (Durabond 954 loaded with steel, from Cotronics).

2.2. Characterization of catalysts and of catalytic membranes

The X-ray diffraction (XRD) patterns ($2\theta = 5°$–$125°$) of powder samples were obtained by using a diffractometer (Inel CPS 120) equipped with a copper anticathode (Cu $K\alpha_1 = 1.5406$ Å) and a curved detector.

The surface area measurements by nitrogen adsorption were carried out using the multipoint BET method, after degassing the sample 3 h at 250 °C under nitrogen. The mean size of catalyst grains suspended in ethylene glycol was measured with a laser granulometer (Galaï CIS-1). The pore size distribution of the membrane was measured with a mercury porosimeter (Micromeritics 9320). Two series of measurements allowed the high (<100 μm) and low (<0.01 μm) pore size ranges to be covered.

The reducibility and reoxidability of the catalyst were studied by thermogravimetry on a Setaram mtb10^{-8} microbalance at 6 °C min^{-1} and with 3 l h^{-1} STP flow rates. The powder sample (30–35 mg) was reduced with diluted hydrogen ($N_2/H_2 = 70/30$) and reoxidized with diluted oxygen ($N_2/O_2 = 85/15$).

Table 1
Composition and operating conditions during preparation of catalysts.

Catalyst	Composition	Preparation method	Sintering temp. (°C)	Step time (h)
BiEuO	$(Bi_2O_3)_{0.7}$–$(Eu_2O_3)_{0.3}$	Mechanical	800, 1000	10, 24
BiErO	$(Bi_2O_3)_{0.75}$–$(Er_2O_3)_{0.25}$	mixing	850	4
BiVO	$(Bi_2O_3)_{0.85}$–$(V_2O_5)_{0.15}$	of oxides	850	10
BiNbO	$(Bi_2O_3)_{0.85}$–$(Nb_2O_5)_{0.15}$		900	10
BiLaO	$(Bi_2O_3)_{0.85}$–$(La_2O_3)_{0.15}$	Co-precipitation	290, 425, 800	4, 16, 16
$BiCe_{0.1}O_y$	$(Bi_2O_3)_{0.83}$–$(CeO_2)_{0.17}$	from aqueous	290, 425, 800	4, 16, 16
$BiCe_{0.33}O_y$	$(Bi_2O_3)_{0.75}$–$(CeO_2)_{0.50}$	nitrate	290, 425, 800	4, 16, 16
$BiCeO_y$	$(Bi_2O_3)_{0.33}$–$(CeO_2)_{0.67}$	solutions	290, 425, 800	4, 16, 16

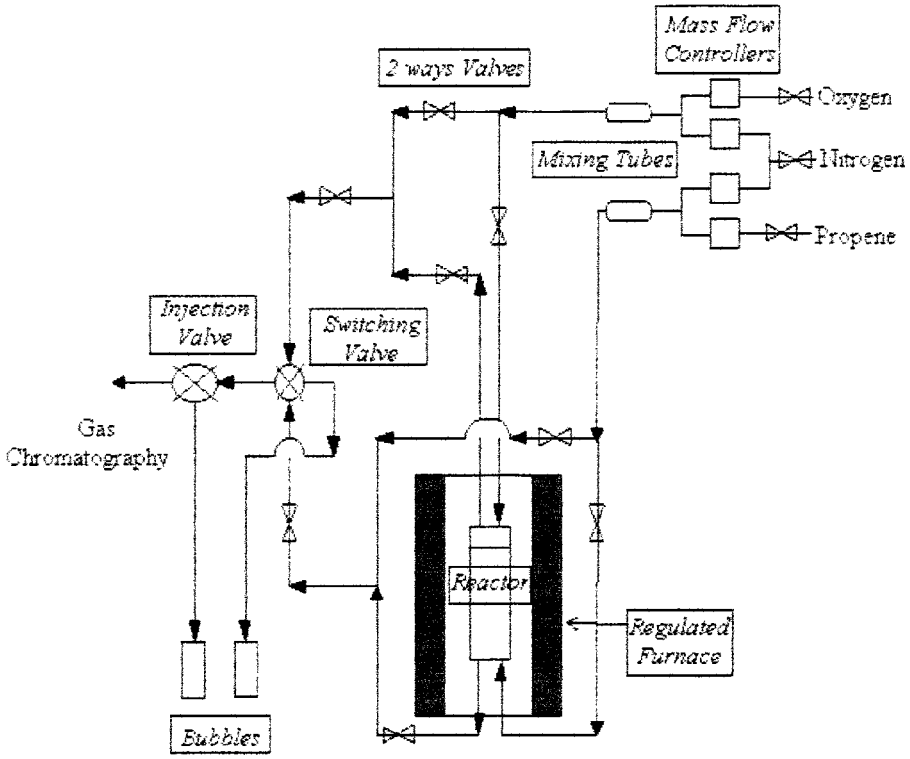

Figure 2. Catalytic bench-scale apparatus.

When data were not available in literature, the electric conductivity σ was measured by impedance spectroscopy. The disk was placed as a solid electrolyte between an electrode and a counter-electrode. The impedance variation of this circuit was studied vs. frequency, which was varied between 1 Hz and 1 MHz by means of a frequency analyst (Solartron SI 1255).

The surface of the membrane before and after catalytic reaction (reaction side and oxidation side) was examined by scanning electronic microscopy (JSM 840) and X-ray emission spectrometry to determine the sample composition.

2.3. Catalytic reactor and operating conditions

The configuration of the stainless-steel membrane reactor (figure 2) was inspired from the work by Di Cosimo et al. [9]. Two reaction chambers were separated by the membrane disk which was sealed on the inconel sample carrier. Inlet gas flows of propene/N_2 20/80 and O_2/N_2 (from 10/90 to 40/60) were controlled with mass flow controllers. The reactor was placed in a tubular furnace and connected to the catalytic bench scale test (figure 2). The effluents were analyzed on-line by gas chromatography (Varian GC3300 equipped with TCD). When oxygen was fed on the oxidation side, no oxygen could be detected on the reaction side, and conversely, propene fed on the reaction side was not detected on the oxidation side. The total gas flow on each membrane side was 0.216 $l\,h^{-1}$ STP at 1 bar. The partial pressure of O_2 was made to vary in the range 0.05–0.5 bar on the oxidation side, while the partial pressure of C_3H_6 was maintained at 0.20 bar on the reaction side. The conversion of reactants was determined in the temperature range of 400–600 °C. Conversion of propene, selectivities and yields in benzene, 1,5-hexadiene, ethylene and carbon oxides were expressed in mol%.

3. Results

3.1. Structural and textural properties

Solid solutions of the promoter oxide in Bi_2O_3 were expected to form, but sometimes the XRD patterns of the obtained solids show that additional phases, like fcc δ-Bi_2O_3 or cc γ-Bi_2O_3, are detected (table 2). In the case of cerium-containing oxides (Ce/Bi = 0.1–1/1), the XRD patterns were identified by comparison with β-Bi_2O_3. No cerium oxide (Ce_2O_3 or CeO_2) was detected and a solid solution of β-Bi_2O_3 type was supposed to form. The δ form of Bi_2O_3 was found as a secondary phase but the presence of $Bi_4V_2O_{11}$ could not be ascertained [23].

All specific surface areas (table 2) are lower than 1 $m^2\,g^{-1}$, as expected from the high temperature of sintering. As generally observed, the lower the specific surface, the larger the size of grains is (case of BiVO), and conversely (case of BiLaO). The specific surface area before compression (0.54 $m^2\,g^{-1}$) and the mean grain diameter (5.3 μm) of a BiLaO membrane is typical of our catalysts. The porosity of the BiLaO membrane prepared by co-precipitation has been measured. The distribution of the porous volume vs. mean pore diameter is monomodal and

Table 2
Identification of phases by XRD and textural characteristics of catalysts.

Catalyst	x[a]	Main phase	Secondary phase	Ref.	Surface area ($m^2\,g^{-1}$)	d_{50}[b] (μm)
BiLaO	0.15	$Bi_{1.648}La_{0.352}O_3$ hexagonal		[31]	0.5	5.3
$BiCe_{0.1}O_y$	0.17	β-Bi_2O_3 tetragonal solid solution	γ-Bi_2O_3 cc		0.4	5.4
$BiCeO_y$	0.67	β-Bi_2O_3 tetragonal solid solution	–		0.7	7.0
BiEuO	0.30	$Bi_{1.25}Eu_{0.75}O_3$ cubic	$Bi_{1.212}Eu_{0.788}O_3$ cubic + $Bi_2O_{2.33}$ tetrag.	[27]	0.2	5.2
BiErO	0.25	$Bi_{1.5}Er_{0.5}O_3$ cubic	Er_2O_3 cubic	[31]	0.3	7.5
BiVO	0.15	$Bi_{1.7}V_{0.3}O_{3.3}$ monoclinic	δ-Bi_2O_3 fcc	[29] [32]	0.1	10.7
BiNbO	0.15	$Bi_{1.7}Nb_{0.3}O_{3.3}$ cubic	–	[29]	0.2	6.0

[a] x as $(Bi_2O_3)_{1-x}$–$(M_yO_z)_x$.
[b] Mean grain diameter.

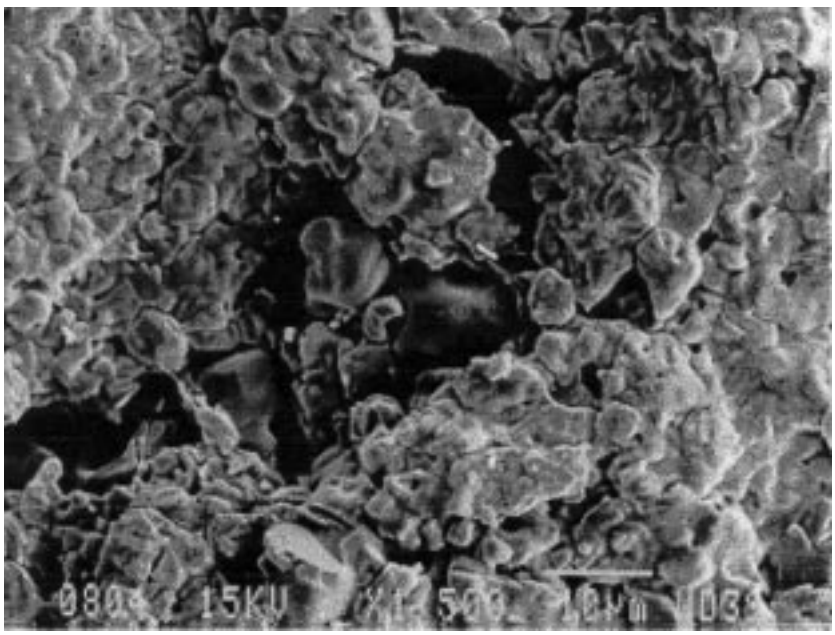

Figure 3. SEM image of the membrane surface before catalytic test (×12,500).

the mean pore diameter amounts to 0.5 μm. This porosity is certainly intergranular because the specific surface area is very low.

Two series of pictures were observed by SEM according to whether the membrane had been used in catalysis or not. Taking again BiLaO as a representative sample, the micrographs before catalysis show that the surface is smooth and constituted by sealed particles after sintering at 800 °C. Some particles, the size of which is close to that measured by laser granulometry (5 μm), can be distinguished too (figure 3). Pores with various sizes (0.25–4.5 μm diameter) are seen at higher magnification (figure 4), in agreement with the mean pore diameter found by porosimetry (0.5 μm). Cracks of few microns wide (figure 3) are also observed. X-ray emission analysis shows that bismuth, lanthanum and oxygen are present in the same proportions throughout the analyzed area, confirming the homogeneity of the sample. After catalysis, on the oxidation side, the surface appearance has changed: separated grains are more numerous and small particles look as if they were dropped onto the surface (figure 5). However, according to X-ray emission, these particles have the same composition as the surface. On the reaction side also the surface looks different. Small aggregated particles are observed, as well as spherical particles on the surface or in the membrane upper layer (figure 6). Pure metallic bismuth is identified in spherules. The presence of Bi, La and O is checked but the proportion of La is far higher than the initial one. Very probably, after the reduction of Bi^{3+} and the migration of Bi^0 towards the surface, lanthanum oxide domains are formed which are not detected by XRD because of their small size.

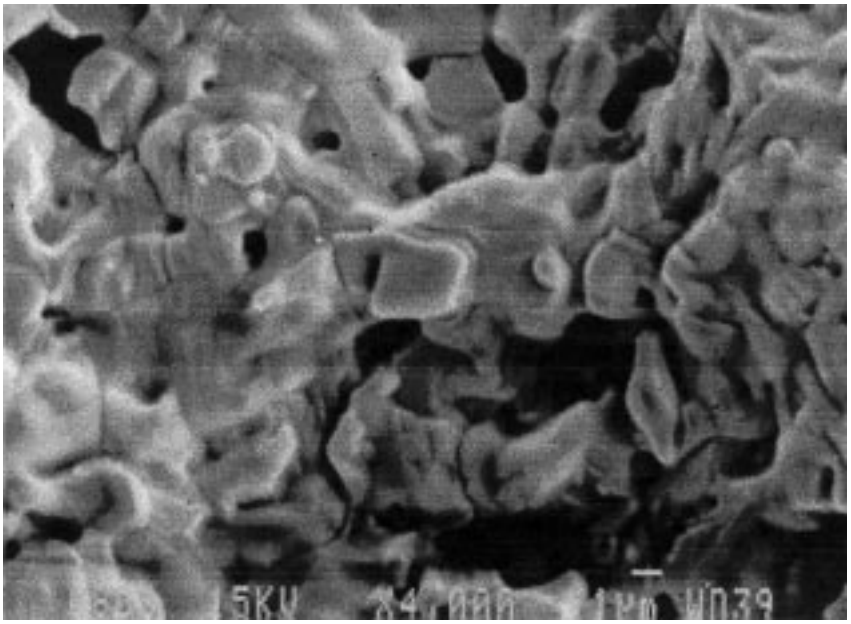

Figure 4. SEM image of the membrane surface before catalytic test (×4,000).

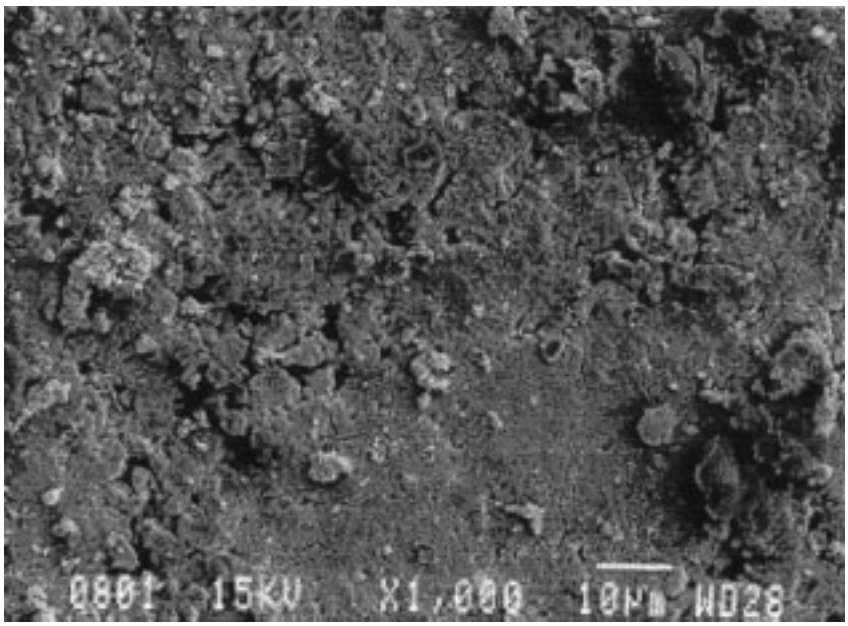

Figure 5. SEM image of the oxidized side of the membrane after catalysis (×1,000).

The electric conductivity σ was measured for $BiCe_{0.1}O_y$ and BiVO at 600 °C or taken from literature data (table 3). The highest conductivity is found for BiErO while the lowest values are obtained for pure Bi_2O_3 forms which are stable at 600 °C. The most effective conductors exhibit a cubic or rhombohedral structure (BiLaO). The ionic contribution of the electric conductivity is expressed by $E/E_0 = \sigma_i/(\sigma_i+\sigma_e)$, where E is the measured f.e.m, E_0 its standard value, σ_i the ionic conductivity, σ_e the electronic conductivity. According to whether the conductivity is essentially electronic or ionic, the ratio E/E_0 is respectively close to 0 or 1. Except the case of α-Bi_2O_3 which is mostly an electronic conductor, all the solids known in literature, including the other forms of Bi_2O_3, are ionic conductors. The E/E_0 ratio varies, according to the oxides and the temperature, between 0.96 and 1 [26,30,31].

3.2. Reactivity of catalysts: reducibility and reoxidability

The reducibility and reoxidability of the doped bismuth oxides before catalysis was examined by thermogravimetry and compared with that of pure Bi_2O_3. The behavior of various samples is compared in terms of temperature at maximum rate of reduction (T_R) and (re)oxidation (T_O), maximum reaction rate (% min^{-1}) and extent of transformation.

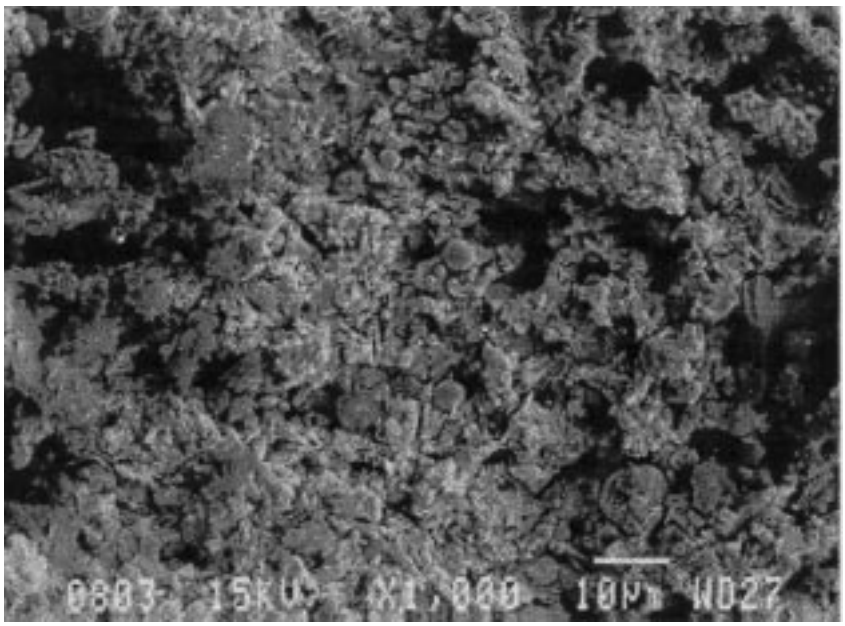

Figure 6. SEM image of the reduced side of the membrane after catalysis (×1,000).

Table 3
Electric conductivity of catalysts measured at 600 °C.

Catalyst BiMO	Conductivity σ (Ω^{-1} cm^{-1})	Reference
α-Bi_2O_3	5×10^{-4}	[26]
β-Bi_2O_3	8×10^{-4}	[26]
γ-Bi_2O_3	3×10^{-3}	[26]
BiLaO	8×10^{-2}	[31]
$BiCe_{0.1}O_y$	1.2×10^{-4}	This work
$BiCeO_y$	2.5×10^{-3}	This work
BiEuO	7.3×10^{-3}	This work
BiErO	1×10^{-1}	[31]
BiVO	1.5×10^{-3}	This work
BiNbO	7×10^{-2}	[29]

Lanthanide promoters accelerate the reduction (figure 7). Indeed, T_R is much lower for Ln-containing Bi_2O_3 (130–230 °C less) than for pure Bi_2O_3 and the reaction rates are greater (from 0.70 to 0.92% min^{-1} instead of 0.36% min^{-1} for Bi_2O_3). For Ln–Bi_2O_3, the experimental weight loss corresponds to the reduction of Bi_2O_3 to Bi^0 showing that the dopant itself is not reduced. This hypothesis is supported by the fact that pure Ln_2O_3 did not present any significant weight loss at 700 °C in the same conditions. Contrary to Ln, Nb and V hinder the reduction which proceeds at 80–100 °C higher than for pure Bi_2O_3. As shown by the weight loss, the dopant is partially reduced, pure V_2O_5 being reduced to V_2O_3 at 520 °C. The reduction rate of BiCeO depends on the cerium content. When it increases, T_R decreases and the reduction is faster (0.89–0.95% min^{-1}) compared to that of pure Bi_2O_3 (0.36% min^{-1}), while pure CeO_2 is not reduced before 700 °C (figure 8). The curves clearly show that the higher the cerium content, the lower the weight loss is, in accordance with the hypothesis that only bismuth is reduced.

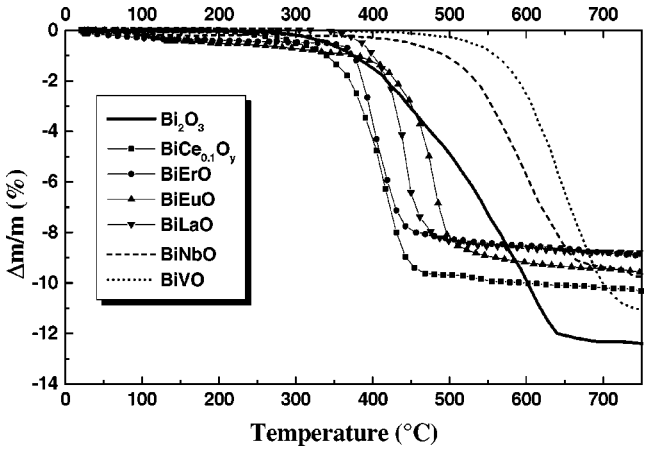

Figure 7. Influence of dopants on the reduction of Bi_2O_3 (TGA).

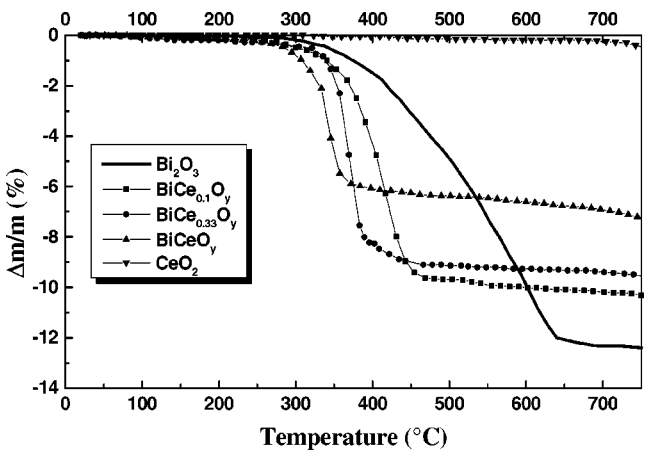

Figure 8. Influence of the cerium content on the reduction of Bi_2O_3 (TGA).

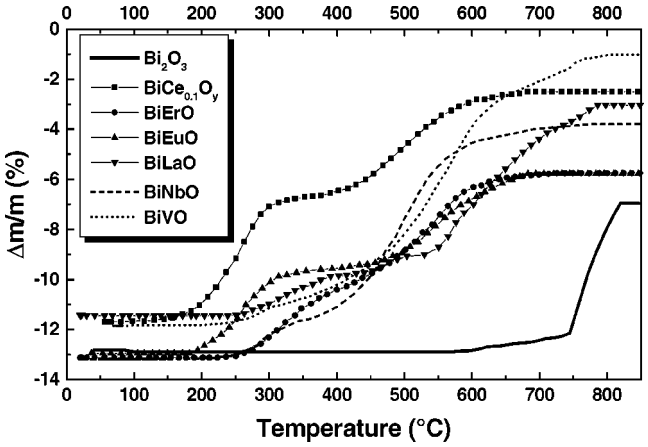

Figure 9. Influence of dopants on the reoxidation of Bi_2O_3 (TGA).

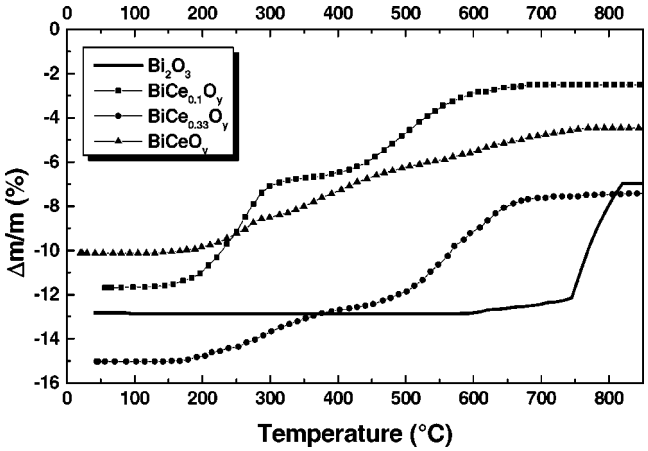

Figure 10. Influence of the cerium content on the reoxidation of Bi_2O_3 (TGA).

The reoxidation of doped catalysts proceeds by two steps at lower rate and temperature than reduction (figure 9). Pre-reduced Bi_2O_3 (to Bi^0) is not fully reoxidized even at high temperature ($T_O = 775\,°C$), as shown by the gain of weight which corresponds to the oxidation of Bi^0 to Bi^{2+}. The second step $Bi^{2+} \rightarrow Bi^{3+}$ proceeds at 850 °C. Reduced BiLnO are reoxidized in two steps, $Bi^0 \rightarrow Bi^{2+}$ and $Bi^{2+} \rightarrow Bi^{3+}$. The effect of all dopants is to decrease strongly the temperature of the second step, from 850 °C with pure Bi_2O_3 to 500 °C on the average. In the case of V and Nb, both the (reduced) dopant and the bismuth are partly reoxidized. The reoxidation of bismuth takes place at lower temperatures ($T_O = 476\,°C$ with Nb and 560 °C with V) than in pure Bi_2O_3, and BiLnO are reoxidized at ca. 460 °C. In the case of Ce-doped oxides, even a low cerium content promotes the reoxidation, which starts at very low temperature (44 °C) for $BiCeO_y$ (figure 10). The rates decrease with increasing cerium content. The weight gain corresponds to the same amount of bismuth which was concerned during reduction, showing again that no cerium was reduced.

To summarize, the dopant is responsible for the increased reactivity of bismuth oxide. If Ln increase both rates of reduction and reoxidation, V and Nb increase only the rate of reoxidation of Bi^0 to Bi^{2+} and Bi^{3+}.

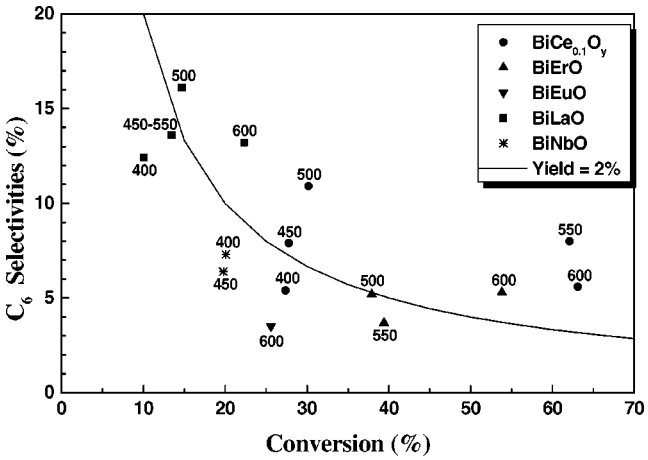

Figure 11. Selectivity to C_6-dimers vs. conversion of propene at various temperatures. Solid line: iso yield of C_6-dimers (2 mol%); numbers indicate reaction temperatures.

3.3. Catalytic properties

In the catalytic membrane reactor, the reactants (propene and oxygen) diluted in nitrogen are separated by the catalytic membrane. Propene is oxidized on one side (reaction side), and oxygen fed on the other side (oxidation side) is supposed to refill the vacancies which are created on the reaction side. The expected reaction products of the oxidative coupling of propene are 1,5-hexadiene and benzene (called C_6-dimers). At constant feed flows, the influence of operating parameters like the temperature of reaction and the oxygen partial pressure (oxidation side) on catalytic properties has been examined for doped catalysts.

Studies of the stability on-stream were first performed at $p_{O_2} = 20$ and 40% on BiLaO. The steady state is reached after 2 h, the figures being stable for 60 h at 550 °C. During the first 2 h, propene conversion and selectivity to CO_2 decrease while selectivity to ethylene increases. Selectivity to C_6-dimers remains low. Bismuth oxide was found not stable enough (reduction to Bi^0 occurred almost immediately) and BiVO yielded only carbon oxides and ethylene.

At fixed $p_{O_2} = 40\%$ in the oxidation side, temperature was made to vary on the same sample (figures 11 and 12). Depending on the promoter, the conversion of propylene ranges from 10 to 65% at 450–600 °C and increases with temperature. Typically, the selectivities to C_6-dimers are low (3–17 mol%), while selectivity to ethylene is close to 30 mol%. The remaining part is carbon oxides, the CO_2/CO ratio being close to 6–7/1. The formation of ethylene and CO_2 by degradative oxidation of propene is observed with all catalysts, including BiVO. No acrolein or other oxygenated products are detected. Above 500 °C, the formation of benzene is promoted at the 1,5-hexadiene expense, from which it is inferred that C_6H_6 is a secondary product. Yields to C_6-dimers are low (1–5 mol%). The most selective catalyst to C_6-dimers is La-doped bismuth oxide (figure 11)

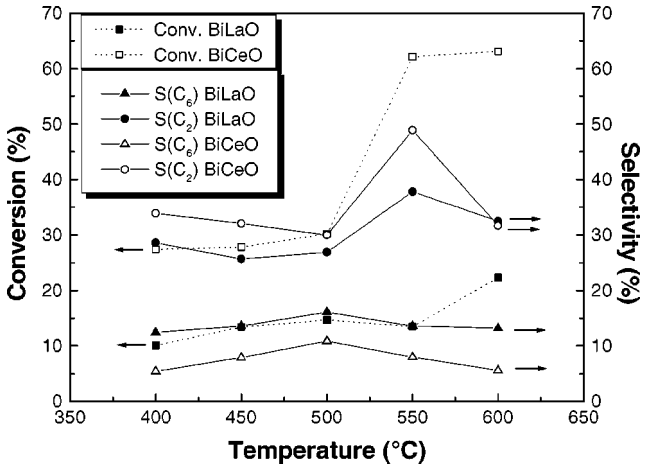

Figure 12. Propene conversion and selectivity to C_6-dimers and other products vs. temperature for BiLaO and $BiCe_{0.1}O$.

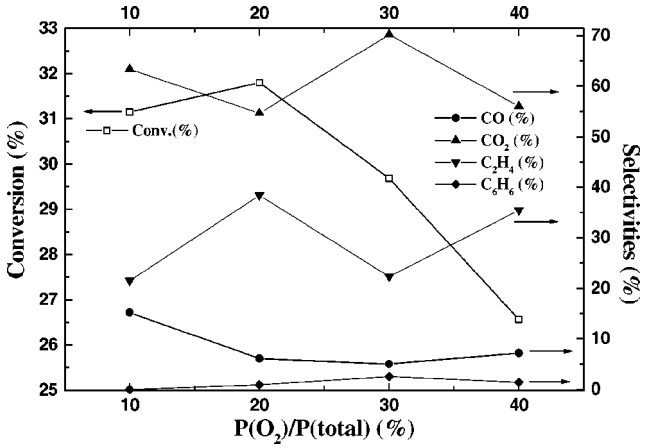

Figure 13. Influence of the partial pressure of oxygen (oxidation side) on propene conversion and selectivity to products for BiLaO at 550 °C.

while BiErO and $BiCe_{0.1}O_y$ are more active. A higher yield is obtained at lower temperature (500–550 °C) with $BiCe_{0.1}O_y$ which is the most active catalyst, but a higher content of Ce is not favorable since no C_6-dimer is found at 500 °C when using Ce/Bi = 1/1. Europium- and niobium-doped catalysts give the lowest yields of C_6-dimers. The influence of temperature on propene conversion is shown in figure 12 for the most interesting catalysts, BiLaO and $BiCe_{0.1}O$. A change of regime occurs between 500 and 550 °C. The increase of conversion corresponds to the decrease of selectivity to C_6-dimers and to an increase of the selectivity to ethylene.

The influence of the partial pressure of oxygen on oxidation side (figure 13) was studied on BiLaO at 550 °C. A new sample was used for each p_{O_2}. The propene conversion decreases slightly with increasing p_{O_2}, all the oxygen being consumed at $p_{O_2} = 10$ and 20%. Higher conversions than in the former experiments (26.6 vs. 14 mol% at 550 °C and 40% O_2) are obtained at steady state but selectivities to C_6-dimers and C_2H_4 are lower (less than 3 mol%) and in a larger range (21–38 mol%), respectively. The production of carbon oxides is not strongly affected.

4. Discussion

It has been shown that the oxidative coupling of propene obeys to the Mars and van Krevelen (1954) mechanism because superficial lattice oxygens O^{2-} participate to the reaction [8,22] and are responsible for selectivity. For a given catalyst, the surface vacancies are replenished either by gaseous dioxygen (when cofed with the reactant) or by bulk O^{2-} oxide ions, depending on the relative rates of these processes [13]. In redox catalysis, the reoxidizing step can be (case of vanadyl pyrophosphate in n-butane oxidation) or not (case of bismuth molybdate in propene oxidation) rate limiting, this behavior determining the state of the solid at the catalytic steady state. In conventional reactors, the cofed oxygen is generally not the limiting reagent, so that the turnover is high enough even when the reoxidation is rate limiting. In the case of catalytic membrane reactors for oxidation, a rate-limiting reoxidation becomes a problem to solve, and the diffusion of oxygen through the membrane must ensure the reoxidation of the reactive surface. Accordingly, it is necessary to know if the ionic diffusion of O^{2-} from bulk to surface is fast enough compared to the eventual molecular diffusion of O_2 through the pores. Therefore, three questions have to be answered: (i) since dopants influence the redox mechanism in non-catalytic conditions, is that redox related or not to the catalytic activity and/or selectivity; (ii) is the ionic conductivity related or not to catalytic properties; and (iii) what is the prevailing mechanism of reoxidation in the CMR.

Taking into account the error made on specific surface area measurement when values lower than 1 $m^2\,g^{-1}$ are obtained (table 2), the texture of the samples is not strongly different so that their reactivity may be directly compared. TGA experiments show that the reduction of LnBiO by hydrogen proceeds at higher temperature than their reoxidation by oxygen, and the same effect is expected with propene [19]. With lanthanides which are more reactive than V and Nb, particularly during reduction, the metallic bismuth formed is reoxidized easily to Bi^{2+} and then to Bi^{3+} at higher temperature. When comparing with catalytic conditions (ca. 450–600 °C) (figures 11 and 12), one can see from thermogravimetric experiments that the reduction is faster than the reoxidation, so that the reoxidation would be the rate-limiting step. Among Ln-doped oxides, BiEuO exhibits the slowest rates of reduction and of reoxidation, in accordance with low propene conversion (25% at 600 °C), contrary to $BiCe_{0.1}O$ which exhibits the higher redox rates and a high conversion of propene (62% at 550 °C). Adding cerium boosts the activity of Bi_2O_3 and allows benzene to be produced at lower temperature, as shown by experiments in conventional pulse reactor [18]. BiLaO is the most selective catalyst to C_6-dimers while giving similar yields as BiErO (at 500 °C) or $BiCe_{0.1}O$ (at 600 °C).

From the ionic conductivity data (table 3), σ is seen to decrease from BiErO (10^{-1} S cm^{-1}) to $BiCe_{0.1}O$ (1.2×10^{-4} S cm^{-1}) along Er > Nb, La > Eu > Ce_1 > $Ce_{0.1}$. What is to be expected in the CMR is that the more con-

ducting, the more active the catalyst because of the higher turnover due to an easier replenishment of oxygen vacancies by O^{2-}. Highly conducting perovskites are good catalysts for the total oxidation of organics and in other reactions like coupling of methane [4], but a direct correlation between ionic conductivity and selectivity has not yet been found. Several reasons could be invoked, but in our case, one of the prevailing could be the texture of the solid which is not properly designed so as to favor a good ionic conductivity. If a simple sintered disk of material allows the determination of the conductivity by electric methods, it is certainly not so in the present case. Another reason is that all the expected, highly conducting phases have not been synthesized, as shown in table 2. Finally, molecular oxygen must be reduced on the surface of the membrane (oxidation side) in order to further diffuse as O^{2-} inside the solid. Therefore, a certain degree of electronic conductivity is necessary. This requirement could not have been met because the solids we examined are mostly ionic conductors [13].

Therefore, it is probable that the prevailing conduction mechanism is not by oxide ions but by molecular diffusion of O_2. Such a diffusion would account for the poor selectivity to C_6-dimers we observe, propene being able to react directly with O_2 so as to yield CO_2. Dioxygen (and nitrogen) could flow through the open pores or cracks created on-stream during the first minutes by the very fast formation of Bi^0, the melting temperature of which is very low (270 °C). The coexistence of solid and liquid domains at reaction temperature increases the influence of diffusion paths on the catalytic reaction, as well as on the replenishment of oxygen vacancies on the reaction side. The experiments performed with BiLaO at various p_{O_2} (oxidation side) but at the same pressure of propene (reaction side) show that, at the steady state, a low partial pressure of oxygen seems to be favorable to the conversion of propene. This behavior is somewhat surprising (figure 13), and since each fresh sample is submitted to one p_{O_2} and experiments are performed at steady state, it cannot be attributed to the evolution of the solid with time. The reproducibility of the catalytic material manufacture ("membrane" disk) is probably questionable, as well as the formation of pores and the creation of diffusion paths in the first 2 h of transient regime.

5. Conclusion

Lanthanides or transition elements doped Bi_2O_3 allow the formation of cubic or rhombohedral oxides having a greater electric, essentially ionic, conductivity than pure Bi_2O_3. The effect of lanthanide dopants on reactivity is to decrease strongly the temperatures of reduction by hydrogen (by 130–230 °C) and of reoxidation (by 300–400 °C) while increasing mostly the rate of reduction. The turnover of the oxidative dimerization of propene is then higher than with undoped Bi_2O_3 but the formation of Bi^0 is not avoided and reoxidation is the rate-limiting step. This characteristic should not be a trouble in a CMR, provided that oxygen is fed in due time to refill the oxygen vacancies produced by the reaction. Because the catalysts are poor electronic conductors, the first step which is the reduction of O_2 to O^{2-} on the oxidation side is too slow, and the oxygen vacancies on the reaction side are not replenished. The texture of our solid samples is not appropriate, not only because of numerous grain boundaries, but also because of the (uncontrolled) porosity due to the formation of liquid droplets of Bi^0. Therefore, the molecular diffusion of dioxygen is prevailing, which accounts for the large amount of carbon oxides formed during the reaction. To progress, the "membrane" state (controlled porosity or dense membrane) of the disks must be improved and the oxygen permeability of the catalysts has to be measured.

Acknowledgement

We gratefully acknowledge the Laboratoire de Cristallochimie et Physicochimie du Solide de l'Ecole Nationale Supérieure de Chimie de Lille for measurements of electric conductivity.

References

[1] J.A. Dalmon, A. Giroir-Fendler, C. Mirodatos and H. Mozzanega, eds., *Catalysis in Membrane Reactor*, Catal. Today 25 (1995).
[2] U. Balachandran, J. Dusek, S.M. Sweeney, R.B. Poeppel, R.L. Mieville, P.S. Maiya, M.S. Kleefish, S. Pei, T.P. Kobylinski, C.A. Udovich and A.C. Bose, Am. Ceram. Bull. 75 (1995) 71.
[3] R. Bredesen, O. Chalvet, H. Roeder, C. Simon and Å. Fjellvag, in: *Proc. 4th Workshop ESF Network – Catalytic Membrane Reactors*, Oslo (1997) p. 181.
[4] S.J. Xu and W.J. Thomson, AIChE J. 43 (1997) 273.
[5] A. Mbandza, Ph.D. thesis, Compiègne (1987).
[6] T. Kompany, Ph.D. thesis, Compiègne (1990).
[7] F. Oudet, A. Véjux, T. Kompany, E. Bordes and P. Courtine, Mater. Res. Bull. 24 (1989) 561.
[8] S. Azgui, F. Guillaume, B. Taouk and E. Bordes, Catal. Today 25 (1995) 291.
[9] R. Di Cosimo, J.D. Burrington and R.K. Grasselli, J. Catal. 102 (1986) 234.
[10] J. Mars and D.W. van Krevelen, Chem. Eng. Sci. 3 (1954) 41.
[11] J.F. Brazdil, R.G. Teller, R.K. Grasselli and E. Kostiner, in: *Solid State Chemistry in Catalysis*, ACS Symp. Series, eds. R.K. Grasselli and J.F. Brazdil, Vol. 279 (Am. Chem. Soc., Washington, DC, 1985) p. 57.
[12] B. Grzybowska, Catal. Today 1 (1987) 341.
[13] P.J. Gellings and H.J.M. Bouwmeester, eds., Catal. Today 12 (1992) 27.
[14] E. Bordes, in: *Elementary Reaction Steps in Heterogeneous Catalysis*, eds. R.W. Joyner and R.A. van Santen (Kluwer Academic, Dordrecht, 1993) p. 137.
[15] P. Subagjo, Ph.D. thesis, Poitiers (1981).
[16] L.M. Kaliberdo, M.I. Tselyutina, A.S. Vaabel, V.M. Kalikhman and B.N. Shvetsov, Russ. J. Phys. Chem. 53 (1979) 843.
[17] M.G. White and J.W. Hightower, J. Catal. 82 (1983) 185.
[18] L. Wang, Y. Duan, Q. Zhao and Y. Wu, Nippon Kagaku Kaishi 3 (1991) 187.
[19] H.E. Swift, J.E. Bozik and J.A. Ondrey, J. Catal. 21 (1971) 212.
[20] E. Ramaroson, G. Blanchard, M. Che and J.M. Tatibouet, Catal. Lett. 15 (1992) 393.
[21] T.P. Snyder and C.G. Hill Jr., Catal. Rev. Sci. Eng. 31 (1989) 43.

[22] V.D. Sokolovski and E.A. Mamedov, Catal. Today 14 (1992) 467.
[23] J.C. Boivin and G. Mairesse, Chem. Mater. 10 (1998) 2870.
[24] A. Cherrak, R. Hubaut, Y. Barbaux and G. Mairesse, Catal. Lett. 15 (1992) 377.
[25] E. Bordes and R.M. Contractor, Topics Catal. 3 (1996) 365.
[26] H.A. Harwig and A.G. Gerards, J. Solid State Chem. 26 (1978) 265.
[27] A.J. Verkerk and M.J. Burggraaf, Solid State Ionics 3/4 (1981) 463.
[28] M.J. Verkerk, K. Keizer and A.J. Burggraaf, J. Appl. Electrochem. 10 (1980) 81.
[29] T. Takahashi, H. Iwahara and T. Esaka, J. Electrochem. Soc. 124 (1977) 1563.
[30] T. Takahashi, T. Esaka and H. Iwahara, J. Solid State Chem. 16 (1976) 317.
[31] H. Iwahara, T. Esaka, T. Sato and T. Takahashi, J. Solid State Chem. 39 (1981) 173.
[32] J.P. Wignacourt, M. Drache and P. Conflant, J. Solid State Chem. 105 (1993) 44.